Science of the Total Environment 635 (2018) 1144–1151

Contents lists available at ScienceDirect

Science of the Total Environment

journal homepage: www.elsevier.com/locate/scitotenv

Light absorption of black carbon is doubled at Mt. Tai and typical urban area in North China

Zhe Bai [a], Xinjian Cui [a], Xinfeng Wang [a], Huijun Xie [a], Bing Chen [a,b,c,*]

[a] Environment Research Institute, Shandong University, Jinan 250100, China
[b] Laboratory for Marine Geology, Qingdao National Laboratory for Marine Science and Technology, Qingdao 266061, China
[c] State Key Laboratory of Cryospheric Sciences, Northwest Institute of Eco-environment and Resources, Chinese Academy of Sciences, Lanzhou 730000, China

HIGHLIGHTS

- BC absorption enhancement was determined by an experimental method that removed aerosol coatings.
- Three thermal-optical methods were evaluated to minimize bias in measurements.
- Mass absorption cross-section of decoated/pure BC was 3.8 $m^2\ g^{-1}$.
- Light absorption was enhanced by a factor of 2 at both urban area and Mt. Tai.
- Coating effect was weakly intensified on regionally aged aerosols at Mt. Tai.

GRAPHICAL ABSTRACT

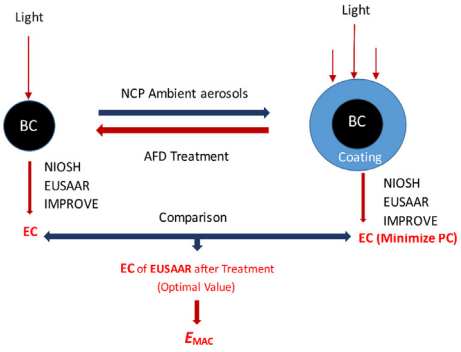

ARTICLE INFO

Article history:
Received 11 March 2018
Received in revised form 17 April 2018
Accepted 18 April 2018
Available online 24 April 2018

Editor: Jianmin Chen

Keywords:
Black carbon
Coating
Mass absorption cross-section
Absorption enhancement
Air pollution

ABSTRACT

The estimates of radiative forcing of black carbon (BC) remain great uncertainty, largely due to variations in the absorption enhancement of BC by mixing with organic and inorganic coatings in ambient aerosols. We applied a two-step solvent treatment method that experimentally removed coating materials in aerosol samples to determine the BC absorption enhancement. Aerosol samples were collected at Mt. Tai and a severely polluted urban area (Jinan) in North China Plain (NCP). The mass absorption cross-section (MAC) of BC aerosols was determined before and after the coating removal. Three thermal-optical protocols, NIOSH, EUSAAR and IMPROVE, were tested for determining of BC mass and MAC. The EUSAAR protocol gave the optimal values of BC mass concentrations and MAC. The MAC for decoated BC was 3.8 ± 0.9 and 3.8 ± 0.1 $m^2\ g^{-1}$ (Average and 1SD) at 678 nm wavelength at the urban area and Mt. Tai, respectively, and it was consistent with the theoretical calculation for pure BC. The MAC for ambient aerosol samples was enhanced to 7.4 ± 2.6 and 7.8 ± 2.7 $m^2\ g^{-1}$ at Jinan and Mt. Tai respectively. Non –BC coatings could enhance the MAC (E_{MAC}) by a factor of 2 at both the polluted urban area and mountain summit. The light absorption of BC may be rapidly enhanced from air pollution in severely polluted area, and then it remains relatively constant for aged aerosols at Mt. Tai. Climate model is recommended for amplifying BC absorption by a factor of 2 in East Asia and other areas with intense industrialization and urbanization.

1. Introduction

Atmospheric black carbon (BC) or element carbon (EC), together with organic carbon (OC) is the main carbonaceous component of fine

* Corresponding author at: Environment Research Institute, Shandong University, Jinan 250100, China.
E-mail address: bingchen@sdu.edu.cn. (B. Chen).

https://doi.org/10.1016/j.scitotenv.2018.04.244
0048-9697/

particulate matter. BC presents strong absorption from the visible to infrared within wavelengths of solar radiation, which has been estimated at large variations from nearly 0 to +1 Wm^{-2} (Bond et al., 2013; IPCC, 2013; Shindell and Fowler, 2012). The absorption of BC can be enhanced from the photochemical production of secondary aerosols or coating effects (Cheng et al., 2017; Liu et al., 2015; Zhang et al., 2018). Climate models estimated that light absorption from BC coating could be amplified by a factor of 1–3 (Chung and Seinfeld, 2005; Flores et al., 2012; Jacobson, 2013). However, several field campaigns have recently observed the BC absorption enhancement <1.5, which only covers the lower limit of the model simulations and theoretical estimations (Bond et al., 2006; Cappa et al., 2012; Jacobson, 2001; Liu et al., 2017).

The mass absorption cross-section (MAC) characterizes the light absorption properties of unit mass of EC (Habib et al., 2008; Schulz et al., 2006). EC mass can be measured with a thermal-optical carbon analyzer with a variety of correction and temperature protocols. Three protocols —NIOSH, EUSAAR, IMPROVE —were generally applied, with their own thermograms yield almost equivalent total carbon (TC) values, while varying EC distributions were recognized across different protocols (Chow et al., 2001; Reisinger et al., 2008). Main reason for disparity includes differences in temperature and the duration time in each step, pyrolyzed carbon (PC, or char), and varying OC/EC split (Vii et al., 2015). The accurate optical correction of PC based on either one of two underlying hypotheses may not hold true since the specific attenuation coefficients of PC is greater than EC (Subramanian et al., 2006), and PC and EC may co-evolve during the oxidization step under Helium/O_2 atmosphere (Cavalli et al., 2010).

In this study, a two-step solvent system was employed to remove non-EC matters in aerosol samples (Cui et al., 2016). This treatment minimized the PC formation during the thermal-optical analysis, and thus lowered the bias in EC measurements. We compared the EC mass before and after the solvent treatment for three thermal-optical protocols to obtain optimal EC. With the corrected EC value, the MAC was calculated for aerosol samples with and without solvent treatment. The solvent treatment meanwhile removed coating matter on BC, and enabled the estimation of the light absorption enhancement of BC from ambient aerosol coatings (Chen et al., 2017a; Chen et al., 2017b). Samples were collected from a severely polluted urban area (Jinan) and Mt. Tai (Taishan) in North China Plain (NCP), representing for relatively fresh aerosols and regionally aged aerosols, respectively.

2. Methods

2.1. Aerosol samples

The samples of fine particulate matter ($PM_{2.5}$) were collected at the Shandong University Monitoring Station (SDUMS, 36.67°N, 117.06°E) in an urban center of Jinan and at the summit of Mt. Tai (1532 m, 36.25°N, 117.101°E). Jinan, as the capital of Shandong Province in the North China Plain, suffered from serious air pollution which was driven by densely population and intense industrialization. Mt. Tai is the highest mountain in the middle of the NCP, and is representative of regionally aged air masses.

$PM_{2.5}$ Samples were collected on 90 mm pre-combusted (600 °C, 4 h) and pre-balanced quartz fibers (Pallflex, Tissuquartz 2500 QAT-UP) mounted on mid-volume (100 L min^{-1}) aerosol cyclone sampler (TH150-A, Wuhan Tianhong INST Group). Thirty aerosol samples were collected during June to July 2016 and July to August 2014 at Jinan (Table S1) and Mt. Tai (Table S2), respectively. The concentrations of water soluble inorganic ions (SO_4^{2-}, NO_3^-, NH_4^+) in $PM_{2.5}$ were measured by a model ADI 2080 online analyzer for Monitoring for AeRosols and Gases (MARGA, Applikon Analytical B.V., the Netherlands) at 1-h time resolution. NO, NO_x, NO_2 (=NO_x − NO), and O_3 were measured by a NO-NO_x analyzer (Thermo, Model 42C) and an O_3 analyzer (Thermo, Model 49C). NO_y is defined as the sum of NO, NO_2, HONO, HO_2NO_2, NO_3, PAN, HNO_3, N_2O_5, aerosol nitrate, and other organic nitrates etc., including nitrate in $PM_{2.5}$. The method of measurement of NO_y was shown in the early studies (Wang et al., 2001; Wang et al., 2010).

2.2. Two-step solvent treatment

The two-step solvent treatment was performed with an aerosol filter filtration-dissolution (AFD) system, which has been developed in our previous study (Chen et al., 2017a). Sample filters were in-situ washed by water and organic solvents to dissolute organic and inorganic matters, and thus BC was isolated and recovered on the sample filter. This BC isolation minimized PC formation that may cause bias on the OC/EC split during thermal-optical OCEC analysis. Moreover, it removed organic and inorganic coatings on the BC aerosols, and enabled to estimate the light absorption enhancement from coating effects of BC-containing aerosols.

2.3. Black carbon measurements with three protocols

A thermal-optical carbon analyzer (Sunset Laboratory, Tigard, OR, USA) was used to determine the elemental carbon (EC, as the mass-based proxy for optical BC) and organic carbon (OC) loadings on the filter. The EC measured by the thermal-optical methods, including thermal-optical transmittance (TOT) and reflectance (TOR), is operationally defined as the carbon that volatilizes from quartz filter samples at elevated temperatures in the presence of oxygen. The three protocols of NIOSH870, EUSAAR-2 and IMPROVE had difference for the temperature steps and TOT or TOR correction (Table S3).

In NIOSH870 program, the oven temperature was first increased to 870 °C in four steps in a pure helium atmosphere to thermally volatilize the OC in the filter samples. Then, the oven temperature was reduced to 550 °C, and an oxygen/helium (10:90) atmosphere was introduced. The oven was heated to 870 °C in six steps, which enabled the thermal oxidization of the EC. The OC might be pyrolyzed (PC) to EC at the first stage in a helium (He) atmosphere, resulting in a decrease in the on-line laser transmission signal, which was monitored through the filter. When entering subsequent oxidized programs to burn the EC and PC, the split point of the two fractions is defined as the point where the laser transmission returned to its initial level before the PC was formed.

IMPROVE utilized reflectance laser for pyrolized carbon (PC) correction instead of the transmittance correction in NOISH (Birch and Cary, 1996; Fung et al., 2004). IMPROVE also differs from NIOSH on the maximum temperature in He phase decreased from 870 °C to 580 °C (Fung et al., 2004).

EUSAAR-2 was derived from NIOSH and IMPROVE, which applied 650 °C as the highest temperature-step in He phase (Cavalli et al., 2010), and the EUSAAR-2 used TOT correction. The differences of temperature steps and laser correction methods influence on the PC correction for OC and EC split. Consequently, the EC concentrations from the three protocol measurements may have large differences.

2.4. Optical properties

A laser beam of carbon analyzer at wavelength 678 nm measured the attenuation (ATN) of aerosols on the filter. The attenuation (ATN) is calculated from the equation:

$$\mathrm{ATN} = -100 \cdot \ln\left(\frac{I}{I_0}\right). \quad (1)$$

where I and I_0 are the transmittance signal before and after the thermal-optical analysis during which EC was burned.

The mass absorption cross-section (MAC) was calculated by the filter loading of EC (μg cm^{-2}) and ATN.

$$MAC = \frac{ATN}{EC \cdot C \cdot R(ATN)} \quad (2)$$

C, is an empirical factor for multiple scattering effect, and a value of C = 5.74 determined with standard vehicle aerosols, was suggested for the filter type, Pallflex, Tissuquartz 2500 QAT-UP (Cui et al., 2016). Another artifact, shadowing effect, related to filter-base method and described by calibration factor R(ATN) was determined by the dependency of optical properties of the deposited particles and the amount of aerosol particles embedded in the filter (Cheng et al., 2011). An increase of ATN correlates well ($R^2 > 0.8$) with EC loading, and the shadowing effect was not identified and R(ATN) = 1 for samples of this study. The BC absorption enhancement due to coatings in ambient aerosols was established by the ratio of MAC before and after the coating removal.

$$E_{MAC} = \frac{MAC_{ORIGINAL}}{MAC_{TREATED}} \quad (3)$$

2.5. Mie theory calculation

The Mie theory on the basis of the shell-and-core model algorithm of Bohren and Huffman (Bohren and Huffman, 1983) was used to calculate optical properties of fresh fractal soot at wavelength of 678 nm. Calculation was made for homogeneous BC particles with diameters between 10 and 100 nm, and with density of 1.8 gcm^{-3}, and refractive index of 1.95–0.79i which theoretically represents BC with little or no voids (Bond and Bergstrom, 2006).

3. Result

3.1. EC concentrations

The EC concentrations of NIOSH (EC_{NIOSH}), EUSAAR (EC_{EUSAAR}), and IMPROVE ($EC_{IMPROVE}$) methods for original samples were 0.9 ± 0.6, 1.5 ± 1.0 and 3.0 ± 1.3 μg m^{-3} in Jinan, respectively, which were higher than those on Mt. Tai (0.5 ± 0.2, 0.7 ± 0.2 and 1.5 ± 0.6 μg m^{-3}). The EC concentrations varied due to the temperature protocol, with NIOSH protocol showed the lowest EC values, while $EC_{IMPROVE}$ was the highest (Fig. 1).

The AFD two-step solvent treatment removed majority OC, and the flat laser signal at the helium stage suggested minimum PC production, which lowered the negative influence on the OC/EC split (Fig. S1). Consequently, the differences among the three protocols were decreased after the AFD treatment. The EC_{EUSSAR} remained almost the same before and after the AFD OC removal. EC_{NIOSH} increased after the AFD treatment, while $EC_{IMPROVE}$ after AFD treatment was only half to the original sample (Fig. 1).

3.2. ATN

The ATN measurements of the original samples were similar among three protocols (ATN_{NIOSH}, ATN_{EUSSAR}, and $ATN_{IMPROVE}$) both at Jinan (87 ± 39, 86 ± 40, 85 ± 40) and Mt. Tai (60 ± 19, 69 ± 22 and 69 ± 22) (Fig. 2). After the two-step treatment, the ATN for NOISH, EUSAAR and IMPROVE were 46 ± 27, 47 ± 25, 47 ± 28 at Jinan and 32 ± 11, 34 ± 13, 37 ± 15 at Mt. Tai, respectively. The treated sample decreased in ATN, which was attributed to absorption enhancement from coating. The three analyzing protocols had influence on EC, while optical measurements were little influenced.

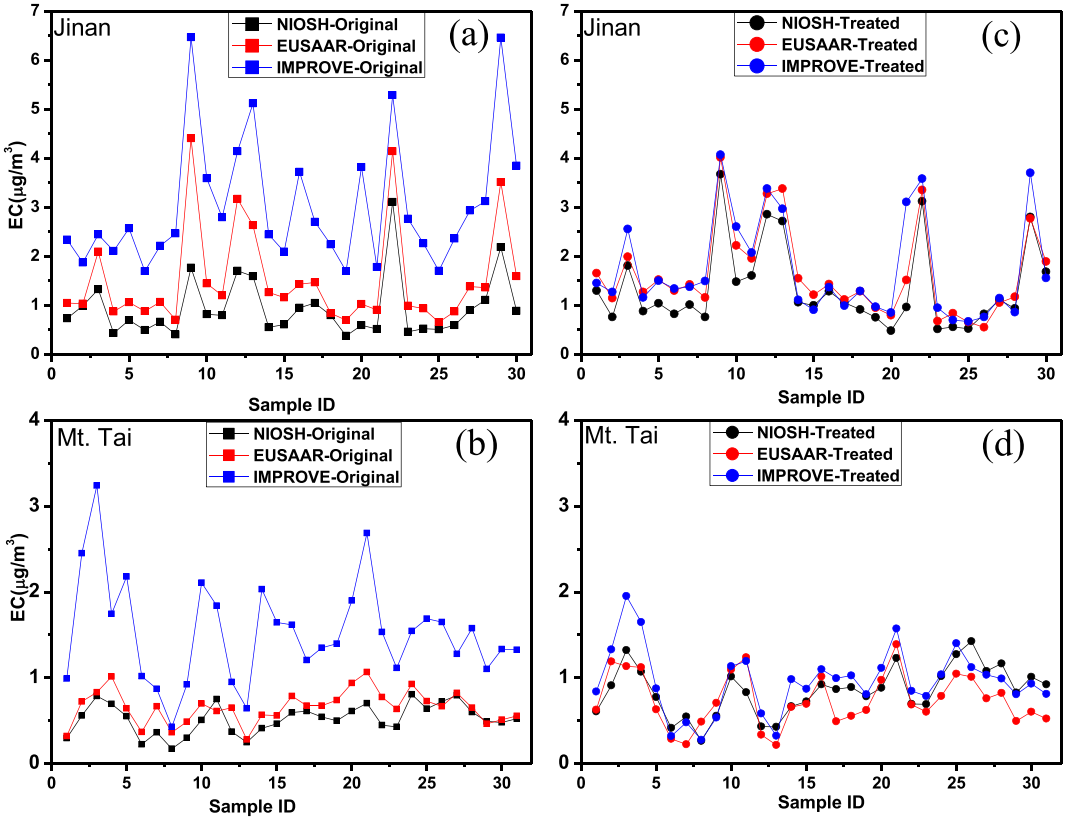

Fig. 1. The EC concentrations measured with three protocols (NIOSH, EUSAAR and IMPROVE) for original samples (a, b) and after the AFD treatment (c, d) at Jinan and Mt. Tai. The sample ID is the same as Table S1 (Jinan), S2 (Mt. Tai).

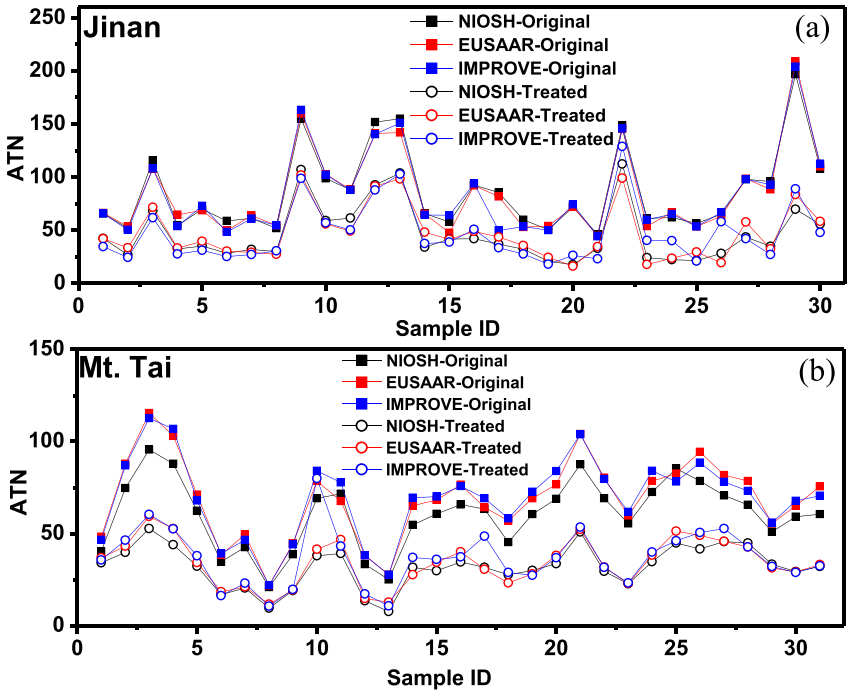

Fig. 2. The ATN of the original samples and after AFD treatment measured by NIOSH, EUSAAR, and IMPROVE protocols for Jinan (a) and Mt. Tai (b).

3.3. Mass abortion cross-section

The MAC at 678 nm of original aerosol samples were 13.1 ± 2.7 (NIOSH), 7.9 ± 1.6 (EUSAAR), and 3.6 ± 0.6 (IMPROVE) $m^2\ g^{-1}$ at Jinan, and 7.4 ± 1.0 (NIOSH), 8.1 ± 1.5 (EUSAAR), and 3.6 ± 0.6 (IMPROVE) $m^2\ g^{-1}$ at Mt. Tai, respectively (Fig. 3). The EC variations in three protocols caused large variations of MAC. After the AFD treatment, the variations of MAC among the three protocols were smaller both at

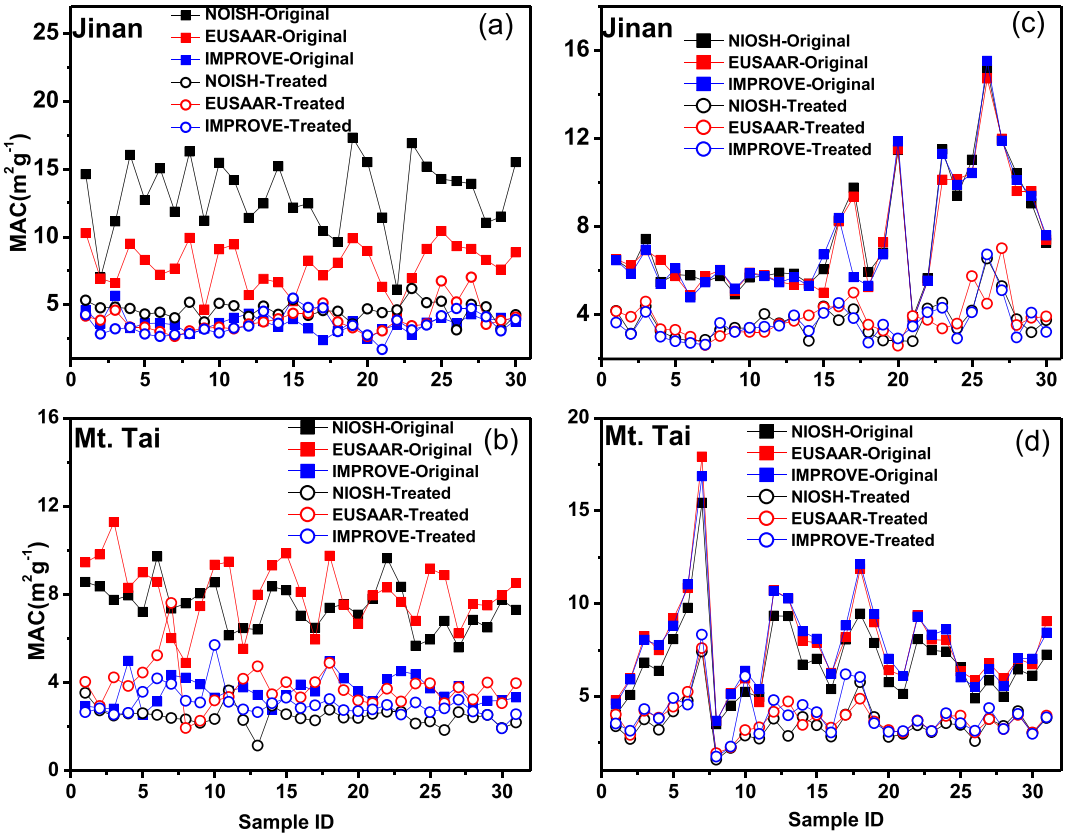

Fig. 3. The MAC calculated before (a, b) and after (c, d) the EC correction.

Jinan (4.6 ± 0.7, 3.9 ± 1.0, and 3.6 ± 0.8 $m^2\ g^{-1}$) and Mt. Tai (2.5 ± 0.4, 3.8 ± 1.0 and 3.0 ± 0.7 $m^2\ g^{-1}$), which can be explained by the relatively accurate measurement of EC after the OC removal.

3.4. Enhancement of MAC

The light absorption enhancement of BC (E_{MAC}) from coating effect was determined by comparing MAC before and after the AFD decoating treatment (Fig. 4). The E_{MAC} of NIOSH resulted in the highest values (2.9 ± 0.7 (Jinan), and 3.1 ± 0.7 (Mt. Tai)), IMPROVE appeared to give lowest data (1.0 ± 0.3 (Jinan) and 1.2 ± 0.3 (Mt. Tai)), and EUSAAR (2.1 ± 0.6 (Jinan) and 2.2 ± 0.6 (Mt. Tai)) showed the moderate. The BC absorption enhancement showed large disparity for the same sample. Therefore, the correction of EC measurements for three analyzing protocols is required.

4. Discussion

4.1. Evaluation of EC for three protocols

Due to minimal pyrolized carbon formation, EC concentrations of the treated filters for three protocols are more strongly correlated to each other ($R^2 = 0.9$, $R^2 = 0.9$, $R^2 = 0.9$) than those of the original samples ($R^2 = 0.9$, $R^2 = 0.8$, $R^2 = 0.7$) (Fig. S2). Meanwhile, the relationship between EC and ATN of the treated samples were higher compared to the original samples for three protocols (Fig. S3). The EC measurements with EUSAAR were in good agreement before and after the treatment. Taken together, we concluded that EUSSAR can get the optimal EC value for samples at Jinan and Mt. Tai, which agree with the hypothesis that EUSAAR is the accurate thermal-optical protocol for measuring EC (Cavalli et al., 2010). It is noted that more investigations should be made before the application of this result to other areas. EC values of NIOSH apparently increased after the AFD treatment, while IMPROVE decreased almost 50% of EC compared with the original samples. The maximum temperature 870 °C of NIOSH in pure He phase is too high to cause light–absorbing substances prematurely evolving in the last He step of this temperature especially when some metal oxides present in sample, leading to inaccurate OC-EC split as Fung et al. (2004) and Chow et al. (2001) reported. Cavalli et al. (2010) show that the maximum 580 °C in He step of IMPROVE protocol do not adequately evaporate all OC, leading to some OC being carried over to He/O_2 phase and thus caused the bias of EC or PC. The EUSAAR protocol favors volatilization of OC and minimizes PC production under the moderate peak temperature (650 °C) and without EC/PC prematurely evolving before the oxidation phase. Taken all together, the EC concentrations of EUSAAR protocol after treatment were recommended for the calculation of MAC for the three protocols.

4.2. Correction of MAC and E_{MAC}

The MAC and E_{MAC} for Jinan and Mt. Tai were recalculated for three protocols by the corrected EC results. The corrected MAC of NIOSH (MAC_{NIOSH}), EUSAAR (MAC_{EUSAAR}) and IMPROVE ($MAC_{IMPROVE}$) for original samples were 7.5 ± 2.7, 7.4 ± 2.6, and 7.4 ± 2.7 $m^2\ g^{-1}$ in Jinan, respectively, which were similar to those on Mt. Tai (6.9 ± 2.3, 7.8 ± 2.7, and 7.9 ± 2.6 $m^2\ g^{-1}$). After the AFD treatment, the corrected MAC_{NIOSH}, MAC_{EUSAAR} and $MAC_{IMPROVE}$ of pure BC were 3.7 ± 0.8, 3.8 ± 0.9, 3.6 ± 0.8 $m^2\ g^{-1}$ in Jinan, and 3.5 ± 1.1, 3.8 ± 0.1, 4.0 ± 1.3 $m^2\ g^{-1}$ on Mt. Tai, respectively (Fig. 3).

The MAC of ambient aerosols for Jinan and Mt. Tai were similar to reports in Beijing winter (8.5 ± 1.7 $m^2\ g^{-1}$) (Cheng et al., 2011), Lhasa (7.2 $m^2\ g^{-1}$) (Li et al., 2016), and Shenzhen (6.5 ± 0.5 $m^2\ g^{-1}$) (Lan

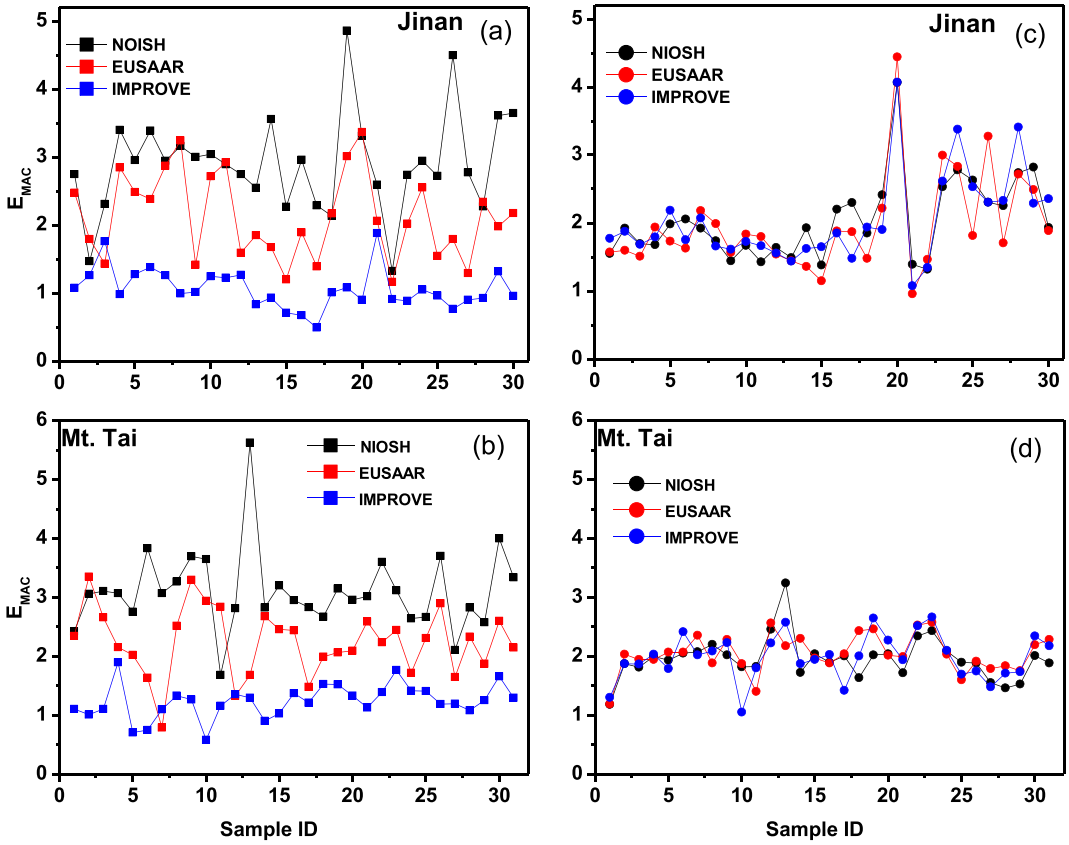

Fig. 4. The E_{MAC} before (a, b) and after correction (c, d) of EC.

et al., 2013). Kirpa Ram (Ram and Sarin, 2009) reported the MAC of 11.3 ± 2.2 (Hisar) and 11.2 ± 2.6 $m^2\ g^{-1}$ (Allahabad) in India, which are higher than that of Jinan (7.4 ± 2.6) and Mt. Tai (7.8 ± 2.7 $m^2\ g^{-1}$) (Table S4). This suggests that MAC of ambient aerosols may have regional variations due to differences in emission sources or coating effects.

The theoretical calculation of MAC for pure BC were in range of 3.9–4.8 $m^2\ g^{-1}$, with the diameter of 10–100 nm (Table S5). The MAC_{EUSAAR} of treated BC in Jinan (3.8 ± 0.9 $m^2\ g^{-1}$) and Mt. Tai (3.8 ± 0.1 $m^2\ g^{-1}$) was close to these theoretical values. The treated sample likely represented pure BC without coatings. The MAC at a wavelength of 530 nm for pure kerosene soot (fresh emission) with a number size distribution peak near 0.3 μm diameter was found to be 7.5 ± 1.2 $m^2\ g^{-1}$ (Bond et al., 2006). In our previous work (Cui et al., 2016), we determined that the MAC of fresh vehicle emission was 5.7 ± 0.67 $m^2\ g^{-1}$ at 678 nm, and after two-step solvent treatment, the MAC of "decoated" BC decreased to 4.0 ± 0.79 $m^2\ g^{-1}$. This suggested light absorption enhancement of fresh emission by co-emitted organic matters. The fresh pure kerosene soot in Bond et al. work contains not only BC, but also co-emitted organic carbon (fresh emission) that may enhance light absorption.

The corrected E_{MAC} were taken by the ratio of corrected MAC. After the correction, the E_{MAC} for the samples from Jinan and Mt. Tai were approximate 2 (Fig. 4). This is close to reports from chamber simulations (2.0) when shell diameter is twice of core (Shiraiwa et al., 2010). Another recent report shows the maximum absorption enhancement (2.4) for BC particles undergoing rapid aging in Beijing within 4.6 h (Peng et al., 2016). They are lower than the E_{MAC} of early ambient observation in Jeju island of South Korea (4.0) (Flowers et al., 2010) (Table S6).

4.3. Constant absorption enhancement for regionally aged aerosols on Mt. Tai

The E_{MAC} on Mt. Tai (2.0 ± 0.3) is only slightly larger that of urban area Jinan (1.9 ± 0.7). The E_{MAC} in the urban area Jinan show considerable correlations with OC/EC ($R^2 = 0.4$). Chan et al. demonstrated that absorption enhancement from coating effect is directly related to the non-refractory mass to BC mass ratio (Chan et al., 2011). Cheng et al. suggested that the MAC of BC generated by biomass burning of controlled combustion in the fire lab is ~7.8 $m^2\ g^{-1}$ (532 nm) when the emission ratios of OC/EC were low (below 0.3) and grows up to 8.8 $m^2\ g^{-1}$ at an OC/EC of 1.2, corresponding to a 13% increase relative to former (Cheng et al., 2016). It is consistent with the results at urban area that E_{MAC} show a trend of growth with the increase in OC/EC ratios. Early study also suggested that E_{MAC} increases rapidly from coating for relatively fresh aerosols at urban area (Chen et al., 2017a).

On the other hand, relative constant E_{MAC} were observed for aged aerosol on Mt. Tai. The backward trajectory analysis suggests that air masses were from different regions during the sampling campaign (Fig. S4 and S5), and thus the sources and atmosphere transportation showed little impact on E_{MAC} variations on the mountain. The E_{MAC} on Mt. Tai display little changes as a function of photochemical age (PCA) (Fig. 5a). Longer PCA on Mt. Tai was accompanied by higher aerosol concentration (Fig. 5b), suggesting the predominance of secondary aerosols on Mt. Tai. We compared the observations from Mt. Tai, rural, and urban campaigns in NCP (Fig. S6). The concentrations of sulfate, nitrate, and ammonium were lower on Mt. Tai than at rural and urban areas in NCP (Fig. 6 a, b, c). The ratios of NO_3^-/EC and NH_4^+/EC showed no obvious difference at the three sites (Fig. 6d, e, f), but SO_4^{2-}/EC ratio was the highest for Mt. Tai. The PCA of Mt. Tai were reasonably larger than those of the urban and rural area in NCP (Fig. 6h, i, g). The diurnal maximum of PCA for $PM_{2.5}$ occurred in the afternoon during which sulfate concentrations peaked. Although sulfate coating continuously formed on aged aerosols on Mt. Tai, the relatively constant E_{MAC} suggests such coating added little value to absorption enhancement for BC. A chamber experiment showed that absorption can be no further enhanced despite continued growth of coating thickness and organic mass (Metcalf et al., 2013). Meanwhile previous studies have suggested that additional absorption enhancement has almost stopped after an extremely thick coating is present on an absorbing core owing to the shell shielding the core from receiving photons (Bond et al., 2006; Cross et al., 2010; Knox et al., 2009; Lack and Cappa, 2010). The observations on Mt. Tai suggested that regionally aged aerosols could maintain BC absorption enhancement at a factor of 2.

5. Conclusion

We applied a two-step solvent treatment method that removed coating materials in aerosol samples to determine the BC absorption enhancement. Three thermal-optical protocols for measurements were evaluated to minimize the bias on EC mass and MAC. The corrected

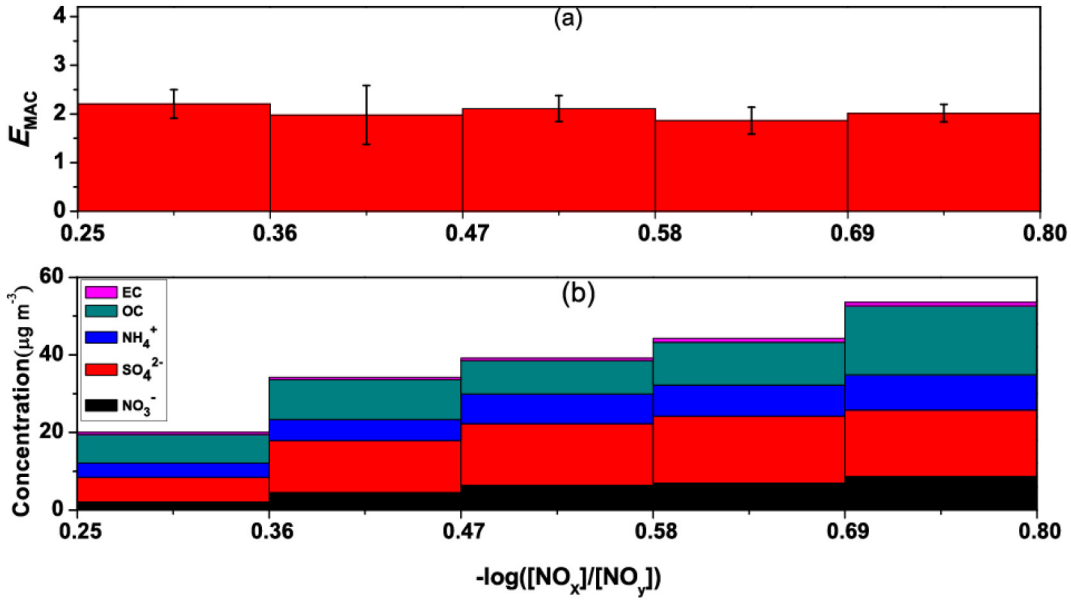

Fig. 5. The average of E_{MAC} (a) and aerosol concentrations (b) as a function of photochemical age (PCA, estimated from –log ([NO_x]/[NO_y]) on Mt. Tai.

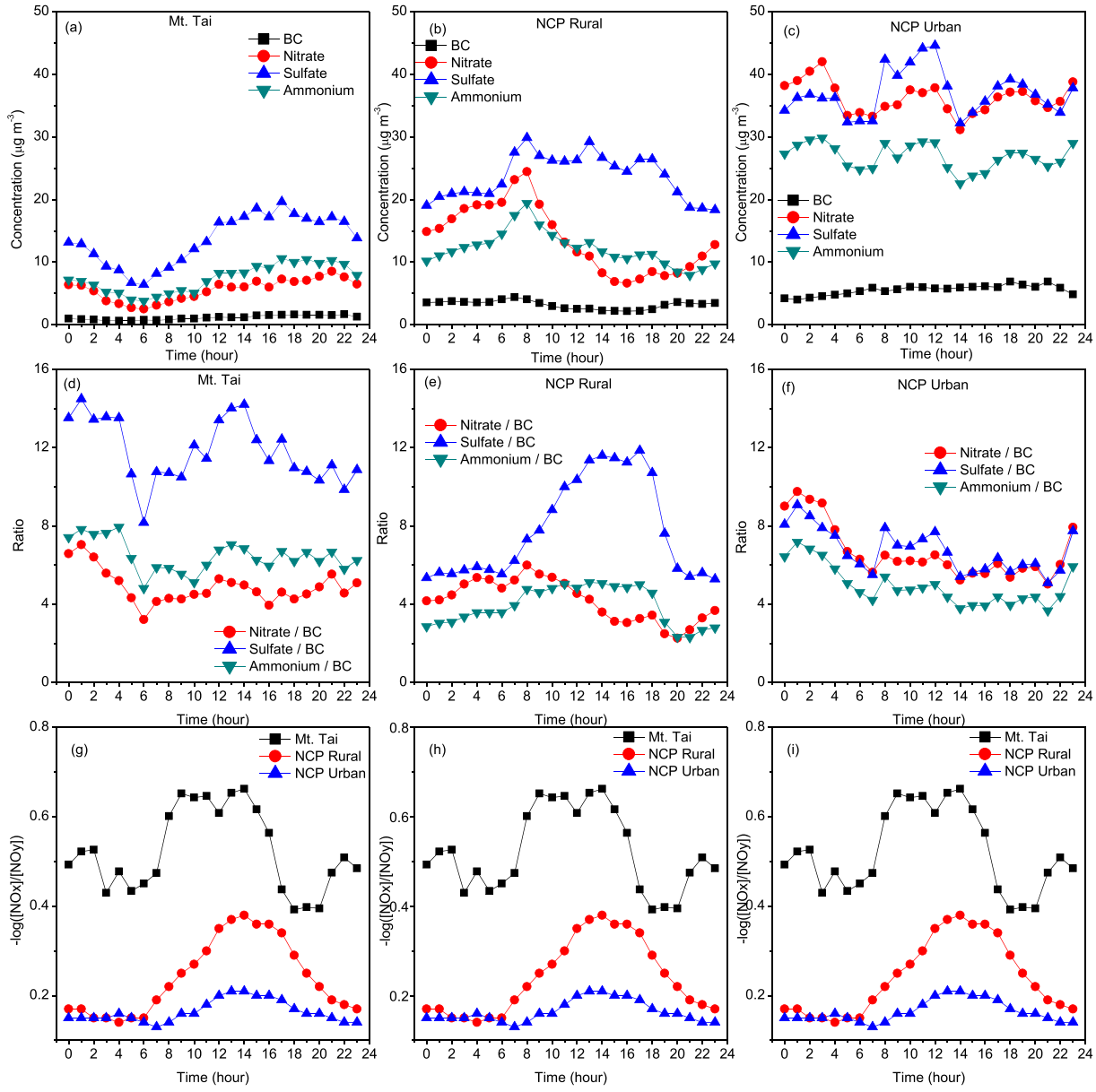

Fig. 6. Mean diurnal patterns for rural (Cui et al., 2016), urban (Chen et al., 2017a) and Mt. Tai campaign in NCP. Concentrations of nitrate, sulfate, and ammonium for $PM_{2.5}$ at Mt. Tai (a), rural (b) and urban area (c). The ratios of NO_3^-/BC, SO_4^{2-}/BC and NH_4^+/BC for Mt. Tai (d), rural (e) and urban (f). -log ($[NO_x]/[NO_y]$) estimated for photochemical aging for Mt. Tai, rural and urban (g, h, i). Please refer Fig. S6 for the three observation sites.

MAC_{EUSAAR} for decoated BC of 3.8 ± 0.9 and 3.8 ± 0.10 m^2 g^{-1} were enhanced to 7.4 ± 2.6 and 7.8 ± 2.7 m^2 $g^{-1}$of coated BC aerosols in urban area (Jinan) and Mt. Tai summer, respectively. The decoated BC had similar MAC between polluted urban area and remote mountain summit, and it was consistent with the theoretical calculation for pure BC. Non–BC coatings on BC core could enhance the light absorption of BC by a factor of 2 (1.9 ± 0.7 for Jinan and 2.0 ± 0.3 for Mt. Tai). E_{MAC} remained constant for aged aerosol on Mt. Tai where air pollution is predominated by secondary aerosols. The observations suggest that climate model can simply amplify the BC radiative forcing by a factor of 2 for both aerosols in urban areas and aged aerosols in remote and background environment.

Acknowledgements

This research has received funding from the National Natural Science Foundation of China (91644214), the Laboratory for Marine Geology - Qingdao National Laboratory for Marine Science and Technology (grant no. MGQNLM-KF201703), State Key Laboratory of Cryospheric Science (SKLCS-OP-2017-01), Taishan Scholars (No. ts201712003) and Key Research and Development Program of Shandong Province (2017GHY215005). The data used are listed in the references, tables, and supplements. The NOAA Air Resources Laboratory (ARL) provided the HYSPLIT transport and dispersion model.

Appendix A. Supplementary data

Supplementary data to this article can be found online at https://doi.org/10.1016/j.scitotenv.2018.04.244.

References

Birch, M.E., Cary, R.A., 1996. Elemental carbon-based method for monitoring occupational exposures to particulate diesel exhaust. Aerosol Sci. Technol. 25, 221–241.
Bohren, C.F., Huffman, D.R., 1983. Absorption and scattering of light by small particles. Wiley Interscience: New York 31 (1), 3.

Bond, T.C., Bergstrom, R.W., 2006. Light absorption by carbonaceous particles: an investigative review. Aerosol Sci. Technol. 40, 27–67.
Bond, T.C., Habib, G., Bergstrom, R.W., 2006. Limitations in the enhancement of visible light absorption due to mixing state. J. Geophys. Res. Atmos. 111, 20211.
Bond, T.C., Doherty, S.J., Fahey, D.W., Forster, P.M., Berntsen, T., Deangelo, B.J., et al., 2013. Bounding the role of black carbon in the climate system: a scientific assessment. J. Geophys. Res. Atmos. 118, 5380–5552.
Cappa, C.D., Onasch, T.B., Massoli, P., Worsnop, D.R., Bates, T.S., Cross, E.S., et al., 2012. Radiative absorption enhancements due to the mixing state of atmospheric black carbon. Science 337, 1078–1081.
Cavalli F, Viana M, Yttri KE, Genberg J. Toward a standardised thermal-optical protocol for measuring atmospheric organic and elemental carbon: the EUSAAR protocol. Atmos. Meas.Tech. 2010; 3: 2321–2345.
Chan, T.W., Brook, J.R., Smallwood, G.J., Lu, G., 2011. Time-resolved measurements of black carbon light absorption enhancement in urban and near-urban locations of Southern Ontario, Canada. Atmos. Chem. Phys. 11, 10407–10432.
Chen, B., Bai, Z., Cui, X., Chen, J., Andersson, A., Gustafsson, O., 2017a. Light absorption enhancement of black carbon from urban haze in Northern China winter. Environ. Pollut. 221, 418–426.
Chen, B., Zhu, Z., Wang, X., Andersson, A., Chen, J., Zhang, Q., et al., 2017b. Reconciling modeling with observations of radiative absorption of black carbon aerosols. J. Geophys. Res. Atmos. 122, 5932–5942.
Cheng, Y., He, K.B., Zheng, M., Duan, F.K., 2011. Mass absorption efficiency of elemental carbon and water-soluble organic carbon in Beijing, China. Atmos. Chem. Phys. 11, 24727–24764.
Cheng, Y., Engling, G., Moosmüller, H., Arnott, W.P., Chen, A.L.W., Wold, C.E., et al., 2016. Light absorption by biomass burning source emissions. Atmos. Environ. 127, 347–354.
Cheng, Y., He, K.B., Engling, G., Weber, R., Liu, J.M., Du, Z.Y., et al., 2017. Brown and black carbon in Beijing aerosol: implications for the effects of brown coating on light absorption by black carbon. Sci. Total Environ. 599-600, 1047–1055.
Chow, J., Watson, J., DaleCrow, Lowenthal D., Merrifield, Thomas, 2001. Comparison of IMPROVE and NIOSH carbon measurements. Aerosol Sci. Technol. 34, 23–34.
Chung, S.H., Seinfeld, J.H., 2005. Climate response of direct radiative forcing of anthropogenic black carbon. J. Geophys. Res. Atmos. 110, 1844–1849.
Cross, E.S., Onasch, T.B., Ahern, A., Wrobel, W., Slowik, J.G., Olfert, J., et al., 2010. Soot particle studies—instrument inter-comparison—project overview. Aerosol Sci. Technol. 44, 592–611.
Cui, X., Wang, X., Yang, L., Chen, B., Chen, J., Andersson, A., et al., 2016. Radiative absorption enhancement from coatings on black carbon aerosols. Sci. Total. Environment 51, 551–552.
Flores, J.M., Baror, R.Z., Bluvshtein, N., Aboriziq, A., Kostinski, A., Borrmann, S., et al., 2012. Absorbing aerosols at high relative humidity: linking hygroscopic growth to optical properties. Atmos. Chem. Phys. 12, 5511–5521.
Flowers, B.A., Dubey, M.K., Mazzoleni, C., Stone, E.A., Schauer, J.J., Kim, S.W., et al., 2010. Optical-chemical-microphysical relationships and closure studies for mixed carbonaceous aerosols observed at Jeju Island; 3-laser photoacoustic spectrometer, particle sizing, and filter analysis. Atmos. Chem. Phys. 10, 10387–10398.
Fung, K., Chow, J., Watson, J., 2004. Factors Contributing to the Difference in Elemental Carbon by the IMPROVE and USEPA Speciation Trends Network (STN) Methods. Proceedings of the 3rd Asian Aerosol Conference, pp. 6–8.
Habib, G., Venkataraman, C., Bond, T.C., Schauer, J.J., 2008. Chemical, microphysical and optical properties of primary particles from the combustion of biomass fuels. Environ. Sci. Technol. 42, 8829–8834.
IPCC, 2013. In: Stocker, T.F., Qin, D., Plattner, G.-K., Tignor, M., Allen, S.K., Boschung, J., et al. (Eds.), Climate Change 2013: The Physical Science Basis. Contribution of Working Group I to the Fifth Assessment Report of the Intergovernmental Panel on Climate Change. Cambridge University Press, Cambridge.
Jacobson, M.Z., 2001. Strong radiative heating due to the mixing state of black carbon in atmospheric aerosols. Nature 409, 695.
Jacobson, M.Z., 2013. Comment on "radiative absorption enhancements due to the mixing state of atmospheric black carbon". Science 339, 393.
Knox, A., Evans, G.J., Brook, J.R., Yao, X., Jeong, C.H., Godri, K.J., et al., 2009. Mass absorption cross-section of ambient black carbon aerosol in relation to chemical age. Aerosol Sci. Technol. 43, 522–532.
Lack, D.A., Cappa, C.D., 2010. Impact of brown and clear carbon on light absorption enhancement, single scatter albedo and absorption wavelength dependence of black carbon. Atmos. Chem. Phys. 10, 4207–4220.
Lan, Z.J., Huang, X.F., Yu, K.Y., Sun, T.L., Zeng, L.W., Hu, M., 2013. Light absorption of black carbon aerosol and its enhancement by mixing state in an urban atmosphere in South China. Atmos. Environ. 69, 118–123.
Li, C., Chen, P., Kang, S., Yan, F., Hu, Z., Qu, B., et al., 2016. Concentrations and light absorption characteristics of carbonaceous aerosol in PM 2.5 and PM 10 of Lhasa city, the Tibetan Plateau. Atmos. Environ. 127, 340–346.
Liu, S., Aiken, A.C., Gorkowski, K., Dubey, M.K., Cappa, C.D., Williams, L.R., et al., 2015. Enhanced light absorption by mixed source black and brown carbon particles in UK winter. Nat. Commun. 6, 8435.
Liu, D., Whitehead, J., Alfarra, M.R., Reyesvillegas, E., Spracklen, D.V., Reddington, C.L., et al., 2017. Black-carbon absorption enhancement in the atmosphere determined by particle mixing state. Nat. Geosci. 10.
Metcalf, A.R., Loza, C.L., Coggon, M.M., Craven, J.S., Jonsson, H.H., Flagan, R.C., et al., 2013. Secondary organic aerosol coating formation and evaporation: chamber studies using black carbon seed aerosol and the single-particle soot photometer. Aerosol Sci. Technol. 47, 326–347.
Peng, J., Hu, M., Guo, S., Du, Z., Zheng, J., Shang, D., et al., 2016. Markedly enhanced absorption and direct radiative forcing of black carbon under polluted urban environments. Proc. Natl. Acad. Sci. 113, 4266–4271.
Ram, K., Sarin, M.M., 2009. Absorption coefficient and site-specific mass absorption efficiency of elemental carbon in aerosols over urban, rural, and high-altitude sites in India. Environ. Sci.Technol. 43, 8233–8239.
Reisinger, P., Wonaschütz, A., Hitzenberger, R., Petzold, A., Bauer, H., Jankowski, N., et al., 2008. Intercomparison of measurement techniques for black or elemental carbon under urban background conditions in wintertime: influence of biomass combustion. Environ. Sci. Technol. 42, 884.
Schulz, M., Textor, C., Kinne, S., Balkanski, Y., Bauer, S., Berntsen, T., et al., 2006. Radiative forcing by aerosols as derived from the AeroCom present-day and pre-industrial simulations. Atmos. Chem. Phys. 6, 5225–5246.
Shiraiwa, M., Kondo, Y., Iwamoto, T., Kita, K., 2010. Amplification of light absorption of black carbon by organic coating. Aerosol Sci. Technol. 44, 46–54.
Shindell, D., Fowler, D., 2012. Simultaneously mitigating near-term climate change and improving human health and food security. Science 335, 183.
Subramanian, R., Khlystov, A.Y., Robinson, A.L., 2006. Effect of peak inert-mode temperature on elemental carbon measured using thermal-optical analysis. Aerosol Sci. Technol. 40, 763–780.
Vii, A.T.B., Pabroa, P.C.B., Santos, F.L., Quirit, L.L., Asis, J.L.B., Dy, M.A.K., et al., 2015. Intercomparison between NIOSH, IMPROVE_A, and EUSAAR_2 protocols: finding an optimal thermal–optical protocol for Philippines OC/EC samples. Atmos. Pollut. Res. 6, 334–342.
Wang, T., Cheung, V.T.F., Anson, M., Li, Y.S., 2001. Ozone and related gaseous pollutants in the boundary layer of eastern China: overview of the recent measurements at a rural site. Geophys. Res. Lett. 28, 2373–2376.
Wang, T., Nie, W., Gao, J., Xue, L.K., Gao, X.M., Wang, X.F., et al., 2010. Air quality during the 2008 Beijing Olympics: secondary pollutants and regional impact. Atmos. Chem. Phys. 10, 7603–7615.
Zhang, Y., Zhang, Q., Cheng, Y., Su, H., Li, H., Li, M., et al., 2018. Amplification of light absorption of black carbon associated with air pollution. Atmos. Chem. Phys. Discuss. 1–27.